Rheophysics of highly concentrated coarseparticle suspensions in a wide gap Couette rheometer

S. Wiederseiner, C. Ancey, M. Rentschler, and N. Andreini

Citation: AIP Conf. Proc. **1145**, 1063 (2009); doi: 10.1063/1.3179828
View online: http://dx.doi.org/10.1063/1.3179828
View Table of Contents: http://proceedings.aip.org/dbt/dbt.jsp?KEY=APCPCS&Volume=1145&Issue=1
Published by the AIP Publishing LLC.

Rheophysics of highly concentrated coarse-particle suspensions in a wide-gap Couette rheometer

S. Wiederseiner, C. Ancey, M. Rentschler and N. Andreini

Laboratoire d'Hydraulique Environnementale, Ecole Polytechnique Fédérale de Lausanne, station 18, CH-1015 Lausanne, Switzerland

Abstract. An optical visualization apparatus has been designed to measure the particle-velocity and solid-concentration profiles of highly concentrated coarse-particle suspensions in a wide-gap Couette rheometer. The main objective is to investigate the frictional-viscous transition, a phenomenon that has been already reported in recent papers [1, 2, 3, 4], but still remains partially understood. For wide-gap viscometers and complex fluids, a related issue is the Couette problem, which underpins the rheometrical treatment for viscometric flows in coaxial-cylinder rheometers; we compare shear-rate computations obtained by solving the Couette problem (bulk estimate) and by differentiating the velocity and concentration profiles (local measurement).

Keywords: Granular matter, non-colloidal suspensions, frictional-collisional transition, rheophysics, fluorescent particle image velocimetry
PACS: 47.57.E-, 45.70.-n, 45.70.Ht, 45.70.Mg

INTRODUCTION

A large number of natural gravity-driven geophysical flows involve suspensions of particles in a fluid. Typical examples include debris flows, snow avalanches, turbidity currents, pyroclastic flows, etc. A longstanding practice is to consider these suspensions as one-phase or two-phase continua on the bulk scale, which makes it possible to use a fluid-mechanics treatment to compute the motion features (velocity, flowdepth, spreading, etc.). The constitutive equation of granular suspensions of particles is known only for limiting flow conditions, where only one type of particle contact prevails. Examples include kinetic theories used to infer motion equations for rapidly sheared flows of particles [5]. In this case, we consider that the main interactions between particles are collisions and the part played by the fluid phase in the generation of stress can be disregarded. Likewise, in the viscous regime the particles interactions are mainly lubricated contacts, in which both the particles and the fluid play a key role. Finally, the frictional behavior exhibited at very low shear rates is usually modeled using the phenomenological law of Coulomb [6, 7]. In this case, it is shown that the bulk stresses result from sustained contacts between particles, which carry frictional forces throughout the bulk [8]; the role of the fluid phase is mainly limited to the fluid pressure in the pores. In many practical cases of interest, the flow regime is intermediate between two limiting regimes; the interplay of two interactions gives rise to more complicated behaviors, which are yet partially understood. For the frictional-viscous transition, Ancey [3] suggested that particle lubrication is the key mechanism. It occurs at a given critical shear rate, which depends a great deal on the particle diameter: at sufficiently high shear rates, fluid inertia increases; part of the fluid can then break and lubricate contacts between particles, which leads to a "fluidization of the material". Another interpretation has been suggested by geophysicists [9]: a concentrated suspension of coarse non-buoyant particles behaves like a soil and according to Coulomb theory, shear strength drops to zero when pore fluid pressure is sufficiently high to balance particle buoyancy forces, which results in a "liquefaction" of the material.

When studying rheological properties of particle suspensions, experimentalists are faced with a number of issues resulting from the presence of particles. For many noncolloidal particle suspensions, the typical particle size is large relative to the standard rheometer gap. In practice, to avoid finite-size effect, a classical approach involves using large-size geometries, e.g., wide-gap Couette cells. For this kind of geometry, the so-called Couette inverse problem has to be solved using specific methods [10, 11, 12, 13, 14, 15] as the thin gap approximation is no longer valid. An alternative way of obtaining the flow curve is to measure the velocity profile across the gap, then differentiate it to derive the local shear rate. The locally derived measurements (shear rate, concentration) can finally be used as benchmark data to test out the various techniques developed for solving the Couette inverse problem (e.g., Tikhonov regularization, spline interpolation, wavelet-vaguelette decomposition). We will present the results of this benchmark.

CP1145, *Powders and Grains 2009, Proceedings of the 6th International Conference on Micromechanics of Granular Media* edited by M. Nakagawa and S. Luding

A CLEAR AND HIGHLY CONCENTRATED COARSE-PARTICLE SUSPENSION

To gain insight into the delicate questions concerning the frictional-viscous transition and the associated Couette inverse problem, we are conducting experiments with an iso-index (clear) particle suspension [16, 17, 18, 19]. The suspensions is made up of spherical PMMA particles of $200\mu m$ within a mixture of three Newtonian miscible fluids to control both the buoyancy forces and refractive index [see Fig.1]. Care must be taken in the preparation of the suspension and the rheometrical experiments to control precisely the fluid temperature because the particle buoyancy and the refractive index matching are strongly dependent of it. To optimize the suspension at the 532 nm used laser wavelength the procedure shown on Fig.2 is performed so as to maximize the transmitted light energy. Tagging the particles with rhodamine 6G, a fluorescent dye, we use a non-invasive fluorescent particle image velocimetry (FPIV) technique to obtain the velocity and concentration profiles.

particle properties

- sphericity
- granulometry
- excellent optical properties

fluid properties

- compatibility with PMMA (wetting and chemical interaction)
- low light absorbtion and excitation

FIGURE 1. Particle suspension properties

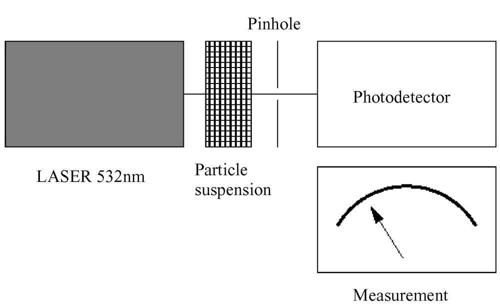

FIGURE 2. Schematic diagram of the turbidity experiment

EXPERIMENTAL FACILITY

The facility is made up of a 2.4-m-long optical table, a second harmonic Nd:YAG laser (532 nm), and a Bohlin Gemini 200 rheometer [see Fig. 3]. The rheometer tools are an inner cylinder or a vane (diameter 25 mm) and an outer quartz cup (60mm in diameter). As shown on Fig. 4, an horizontal laser light sheet cuts the Couette cell at different given heights. The laser light excite the fluorescence of the rhodamine-impregnated particles. The emitted fluorescent light in the 550-nm to 580-nm range is then recorded with a CCD camera at 30 fps. Scattered laser light is blocked by a high-pass optical filter placed in front the camera. Using fluorescent particle image velocimetry (FPIV) and particle tracking techniques (FPTV) to process the images, we finally deduce the velocity and concentration fields.

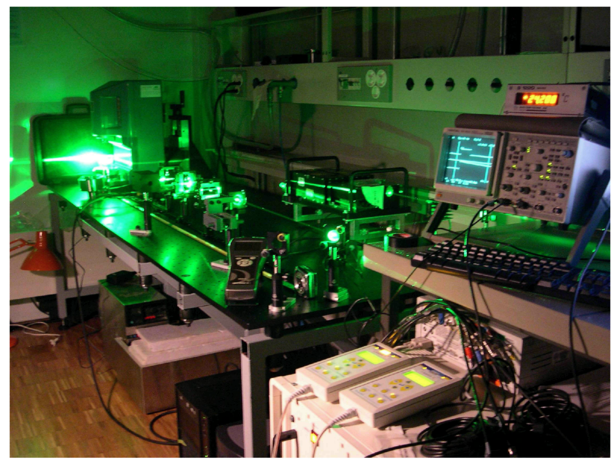

FIGURE 3. the rheo-optical facility

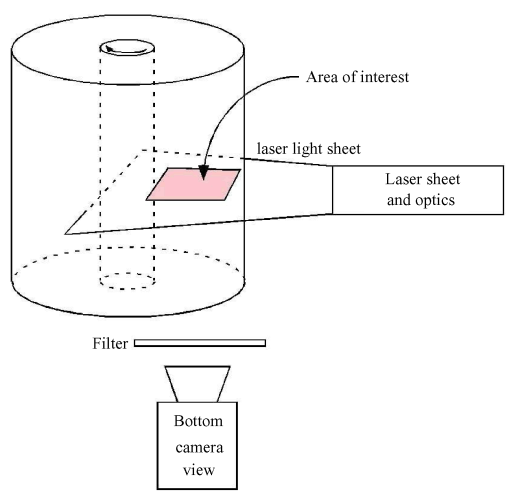

FIGURE 4. sketch of the local measurement technique

PRELIMINARY RESULTS

For validation purpose, we used the Newtonian three-fluid mixture and same PMMA particles as seeding particles for the PIV/PTV treatment. As shown in Fig.

5, good agreement is found for the velocity profiles between the experiment and exact analytical solution. At the moment, experiments with highly concentrated suspensions are in progress.

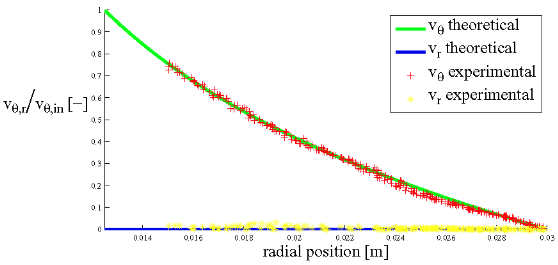

FIGURE 5. Validation velocity profile comparison in the wide-gap Couette cell for a Newtonian fluid, $v_\theta/v_{\theta,in}$ is the non-dimensionalized tangential velocity and $v_r/v_{\theta,in}$ is the non-dimensionalized radial velocity

Some preliminary results with 50% volume fraction and density matched particles suspension (total height $H_T = 50mm$) showed a strong bottom-end effect on the velocity profile. As showed on Fig. 6, even at $0.2H_T$ the velocity profile is still strongly affected by the bottom. In our experiment, we needed to be at about $0.5H_T$ to be rid of the bottom end effect. This probably shows the long distance force chains in highly concentrated particle suspensions. Therefore, a classical methods to obtain the flow curve of highly concentrated suspension will fail, being unable to take correctly into account such a strong bottom-end effect.

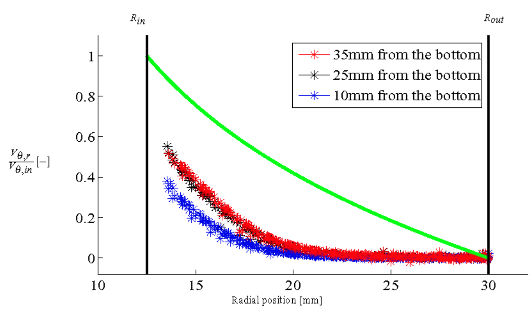

FIGURE 6. Bottom-end effect: tangential velocity profiles at different distances from the tip of the inner cylinder of the Couette cell (we drawed the continuous green line, the theoretical newtonian profile, for comparison)

Fig. 7 shows comparison of the velocity profile derived flow curve and different classical techniques after having reach the steady states. The same qualitative behavior is found but no quantitative agreement.

In Fig. 8 we can see that the shear-induced particle rearranging process is a very slow process taking more than one hour to reach a steady state. Therefore one has to take care to have density matched suspensions to avoid

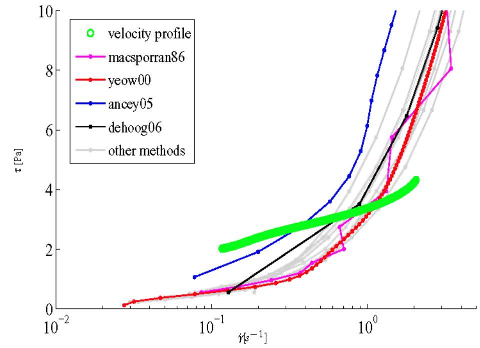

FIGURE 7. Comparison of the bulk calculated flow curves using different solving techniques of the ill-posed Couette inverse problem and the flow curve derived for the velocity profile

to mix up the sedimentation effects with this rearranging processes. Both having then the same time scales.

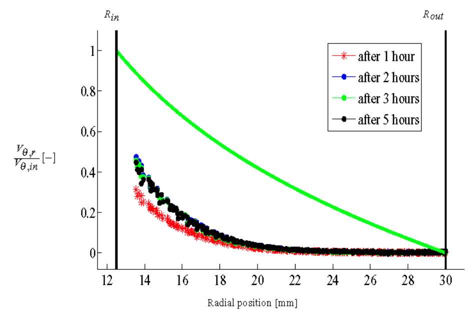

FIGURE 8. Particle migration: evolution of the tangential velocity profile with time (we drawed the continuous green line, the theoretical newtonian profile, for comparison)

ACKNOWLEDGMENTS

The work presented here was supported by the Swiss National Science Foundation under grant number 200021-105193/1 and specific funds provided by EPFL (vice-présidence à la recherche).

REFERENCES

1. D. Prasad, and H. Kytömaa, *International Journal of Multiphase Flow* **21**, 775–785 (1995).
2. C. Ancey, and P. Coussot, *Comptes Rendus de l'Académie des Sciences de Paris* **327**, 515–522 (1999).
3. C. Ancey, *Journal of Rheology* **45**, 1421–1439 (2001).
4. N. Huang, G. Ovarlez, F. Bertrand, S. Rodts, P. Coussot, and D. Bonn, *Physical Review Letters* **94**, 028301 (2005).
5. C. Campbell, *Annual Review of Fluid Mechanics* **22**, 57–92 (1990).

6. G. Mandl, and R. Fernandez-Luque, *Géotechnique* **20**, 277–307 (1970).
7. A. Berker, and W. Van Arsdale, *Rheologica Acta* **31**, 119–138 (1992).
8. F. Radjai, D. Wolf, M. Jean, and J. Moreau, *Physical Review Letters* **90**, 61–64 (1998).
9. R. Iverson, *Reviews of Geophysics* **35**, 245–296 (1997).
10. T. M. T. Yang, and I. M. Krieger, *Journal Of Rheology* **22**, 413–421 (1978), 0148-6055.
11. R. Tanner, and G. Williams, *Transactions of the Society of Rheology* **14**, 19–38 (1970).
12. Q. D. Nguyen, and D. V. Boger, *Annual Review of Fluid Mechanics* **24**, 47–88 (1992).
13. Y. Yeow, W. Ko, and P. Tang, *Journal of Rheology* **44**, 1335–1351 (2000).
14. Y. Leong, and Y. Yeow, *Rheologica Acta* **42**, 365–371 (2003).
15. C. Ancey, *Journal of Rheology* **49**, 441–460 (2005).
16. C. Koh, P. Hookham, and L. Leal, *Journal of Fluid Mechanics* **266**, 1–32 (1994).
17. M. Lyon, and L. Leal, *Journal of Fluid Mechanics* **363**, 25–56 (1998).
18. M. Lyon, and L. Leal, *Journal of Fluid Mechanics* **363**, 57–77 (1998).
19. M. Lenoble, P. Snabre, and B. Pouligny, *Physics of Fluids* **17**, 073303 (2005).